Chemical imaging of interfaces by sum-frequency generation microscopy: Application to patterned self-assembled monolayers

K. Kuhnke,[a] D. M. P. Hoffmann, X. C. Wu, A. M. Bittner, and K. Kern
Max-Planck-Institut für Festkörperforschung, Heisenbergstr. 1, D-70569 Stuttgart, Germany

We demonstrate molecule-specific imaging of a chemically patterned self-assembled monolayer by IR-visible sum-frequency microscopy. The pattern on an Au substrate consists of microcontact printed 10 μm wide alkanethiolate stripes embedded in ω-carboxyalkanethiolate adsorbed from solution. We use both electronic and vibrational contrast mechanisms for a quantitative analysis of thiolate density and the coverage of the two molecular species. The evaluation of images taken at three different IR wavelengths suggests a substantial intermixing of the two thiolates occuring in the preparation procedure. © *2003 American Institute of Physics.* [DOI: 10.1063/1.1624465]

The quantitative analysis of the chemical composition of an interface is a fundamental task in surface and interface science and technology. Chemical groups can be detected by IR spectroscopy even under ambient conditions. Sum-frequency generation (SFG) is a nonlinear and nondestructive method with several appealing properties. It provides both IR and visible spectroscopic information with a high sensitivity to distinguish between ordered and disordered structures. In addition to its inherent time and spatial resolution it has the potential to access buried interfaces with suppressed bulk sensitivity. An optical microscope set-up based on IR-visible SFG allows obtaining chemically specific images from a surface or interface. It is challenging to exploit its potential for a quantitative chemical analysis of a surface with an inscribed chemical pattern using SFG microscopy (SFM). The pattern is formed on an Au substrate by two thiolates with different endgroups; one microcontact printed, the other postadsorbed from solution. In the study we use a home-built sum-frequency generation microscope (SFM). The images yield information on the distribution of different molecular properties. They allow distinguishing between the two molecules and access in a simple way differences of the total molecular density.

We use two 35 ps light pulses, one tunable pulse with $\lambda \approx 3.3$ μm (energy density at the sample: 200 mJ/cm^2) and a $\lambda = 532$ nm pulse (30 mJ/cm^2) at 20 Hz repetition rate generated in a set-up similar to the one in Ref. 1. Both pulses are incident at an angle of $\approx 60°$ from the surface normal and are mixed at the sample surface. The emitted sum-frequency light is employed as a spectroscopic tool for the mid-IR range. The microscope set-up monitors the sample in the generated SFG light. Flörsheimer, Brillert, and Fuchs[2] demonstrated far-field imaging of a LB-monolayer on a fused silica surface by SFM. In that study the observed contrast in a C–H stretching vibration is due to variations of density and molecular orientation in the monolayer. In this article we present contrast due to differences in chemical composition. Our SFM adapted to oblique imaging (60° from surface normal) is described in detail in Ref. 3. It images an area of 250

μm$\times$250 μm with an effective resolution of <3 μm, which is for SFM not restricted by the IR diffraction limit.

The chemically patterned self-assembled monolayer (SAM) is prepared on a 0.2 μm thick polycrystalline Au film. We adsorb octadecanethiol SH–(CH$_2$)$_{17}$–CH$_3$ (in short C17–CH3) by microcontact printing[4,5] with a patterned poly-(dimethylsiloxane) (PDMS) stamp inked with an ethanolic solution (1 mM, contact time 120 s). Then ω-carboxyhexadecanethiol SH–(CH$_2$)$_{15}$–COOH (in short C15–COOH) is adsorbed from ethanolic solution (1 mM, 15 min. immersion time). Both thiolates are sketched in Fig. 1. It is known that the C17–CH3 thiolate forms dense phases with nearly
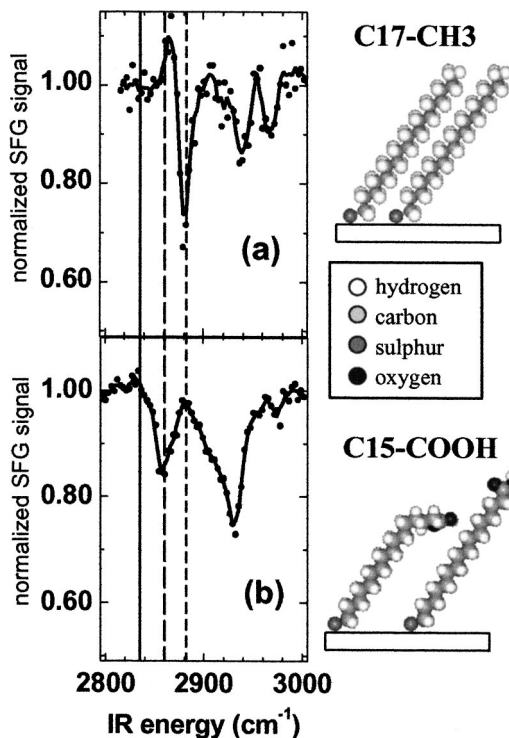

FIG. 1. SFG spectra of homogeneous thiolate layers: (a) Octadecanethiolate monolayer micro-contact printed with a flat PDMS stamp and (b) ω-carboxyhexadecanethiolate monolayer adsorbed from solution. The IR frequencies of the three measurements in Fig. 2 are marked and coded by different dash styles. The molecular structure is sketched in the cartoons on the right.

[a]Author to whom all correspondence should be addressed; electronic mail: k.kuhnke@fkf.mpg.de
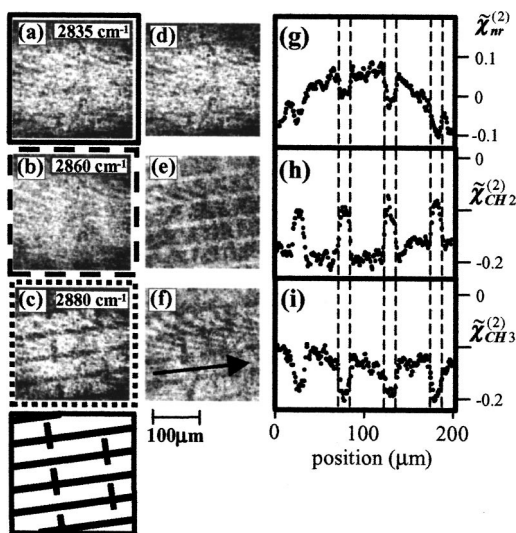
FIG. 2. (a)–(c) Original SFG images at the three IR frequencies marked in Fig. 1: (a) vibrationally nonresonant; (b) at the symmetric methyl stretch; and (c) at the symmetric methylene stretch. The exposure time is 135 min. (d)–(f) Processed images: (d) ''sulfur-image'' obtained using Eq. (4); (e) ''methylene-image'' obtained by pixelwise subtracting image (a) from image (b) using Eq. (5); and (f) ''methyl-image'' obtained by subtracting (a) from (c) using Eq. (5). (g)–(i) Cross sections through the stripe pattern in (d)–(f) with the intensity integrated along to the stripe direction [arrow in (f)]; the contrast is discussed in the text. On the lower left, the printed pattern is shown as it appears in the images.

upright molecular orientation and a coverage of $\approx 1/3$ of the surface Au atom density (Ref. 6 and references therein).

Reference SFG spectra of the pure monolayers of the two thiolates prepared by the same methods as the patterned monolayer are shown in Figs. 1(a) and 1(b). C–H stretching modes appear as negative peaks on a high SFG intensity generated at the thiolate-Au interface. The C17–CH3 thiolate exhibits three methyl resonances, the symmetric vibration and its Fermi resonance at 2880 and 2940 cm^{-1} and the antisymmetric vibrations at 2970 cm^{-1}.[7-10] The C–H stretching modes of the methylene groups in the alkane backbone are not observed because their local inversion symmetry forbids SFG. In contrast, the C15–COOH thiolate does exhibit the symmetric (2860 cm^{-1}) and antisymmetric (2930 cm^{-1}) methylene vibrations. The strength and spectral width of these modes demonstrates the deformation of the alkane backbone [left molecule in the cartoon of Fig. 1(b)], which destroys the local inversion symmetry. From the spectrum which is similar to the one of an amino–amido thiolate[11] we can conclude that the C15–COOH monolayer forms a phase with a bent alkane backbone due to hydrogen bonding between carboxyl groups of adjacent molecules. A vibrational line directly related to the carboxyl group is not observed.

Images of the SAM with the inscribed chemical pattern were taken at three IR frequencies [Figs. 2(a)–2(c)]: 2860 and 2880 cm^{-1} were chosen to provide chemical selectivity to the two thiolates. At these frequencies there is almost no overlap of their vibrational lines (see Fig. 1). The image at 2835 cm^{-1} provides contrast specific to the SFG signal from the Au-thiolate interface and monitors the density of Au-sulfur bonds.

Information on adsorbate distribution is obtained by analyzing the images with respect to their spectral characteristics

at each point of the image. The measured SFG intensity depends on the amplitude of the electric fields of the incoming beams $\vec{E}_i$ and the direction $\vec{e}_{\mathrm{SFG}}$ of the field of the detected SFG radiation

$$I_{\mathrm{SFG}} \propto |\overleftrightarrow{\chi}^{(2)} \vdots \vec{E}_{\mathrm{IR}} \vec{E}_{\mathrm{vis}} \vec{e}_{\mathrm{SFG}}|^2. \tag{1}$$

The $\chi^{(2)}$ tensor describes the second order nonlinear local response of the surface. For fixed geometry it reduces to a complex number. $\chi^{(2)}$ depends on the three photon frequencies involved and, in addition, on adsorbate coverage. SFG spectra from pure Au provide no resonance features in the spectral range analyzed here. Then $\chi^{(2)}$ can be written with nonresonant (nr) and resonant (res) contributions as

$$\chi^{(2)}(\omega_{\mathrm{IR}}, \omega_{\mathrm{vis}}, \omega_{\mathrm{SFG}}) \approx \chi_{\mathrm{nr}}^{(2)} + \chi_{\mathrm{nr}}'^{(2)}(\theta) + \chi_{\mathrm{res}}^{(2)}(\omega_{\mathrm{IR}}, \theta). \tag{2}$$

$\chi_{\mathrm{nr}}^{(2)}$ is about an order of magnitude larger than any of the other contributions on the right-hand side and the latter two can be treated as small quantities

$$I_{\mathrm{SFG,vib}} \propto |\chi_{\mathrm{nr}}^{(2)}|^{(2)} + 2\cos(\phi_1)|\chi_{\mathrm{nr}}^{(2)}||\chi_{\mathrm{nr}}'^{(2)}(\theta)|$$
$$+ 2\cos(\phi_2)|\chi_{\mathrm{nr}}^{(2)}||\chi_{\mathrm{res}}^{(2)}(\omega_{\mathrm{IR}}\theta)|. \tag{3}$$

The first term is a frequency and coverage independent term from the Au surface resulting from interband transitions in Au at the SFG frequency, the second is the coverage-induced change of the signal from the Au-thiolate interface, and the third term represents the vibrational features of the adsorbates. For a SFG intensity I_{nr} measured outside any vibrational transition the third term becomes negligible. By inversion of Eq. (3) for the cases of resonant (res) and non-resonant (nr) images we obtain

$$\tilde{\chi}_{\mathrm{res}}^{(2)}(\theta) = 2\cos(\phi_2)\frac{|\chi_{\mathrm{res}}^{(2)}(\theta)|}{|\chi_{\mathrm{nr}}^{(2)}|} \approx \frac{I_{\mathrm{res}} - I_{\mathrm{nr}}(\theta)}{I_{\mathrm{nr}}(0)}, \tag{4}$$

$$\tilde{\chi}_{\mathrm{nr}}^{(2)}(\theta) = 2\cos(\phi_1)\frac{|\chi_{\mathrm{nr}}'^{(2)}(\theta)|}{|\chi_{\mathrm{nr}}^{(2)}|} \approx \frac{I_{\mathrm{nr}}(\theta)}{I_{\mathrm{nr}}(0)} - 1, \tag{5}$$

which are normalized $\chi^{(2)}$ values that can be used for a chemically specific evaluation. As the clean substrate value $I_{\mathrm{nr}}(0)$ is not directly accessible in the images, we replace $I_{\mathrm{nr}}(0)$ by the average of $I_{\mathrm{nr}}(\theta)$ in the images; this average is <30% smaller than $I_{\mathrm{nr}}(0)$. The factor $2\cos(\phi_i)$ is constant and allows comparing $\tilde{\chi}_{\mathrm{res}}^{(2)}(\theta)$ directly with the normalized peak height in Fig. 1.

Figures 2(d)–2(f) shows the pattern evaluated in a pixel-wise fashion using Eqs. (4) and (5). The contrast in Fig. 2(d) is small indicating a small difference in thiolate coverage; if the two phases had identical densities of sulfur-Au bonds, this contrast would completely vanish. What is surprising is that the contrast observed in Figs. 2(e) and 2(f) is significantly smaller than expected from the spectra of the pure phases. The contrast just gets out of the photon noise in the images (accumulated SFG intensity: ≈ 30 photons/μm^2). The low contrast is a property of the monolayer and not due to the imaging because the large acceptance angle of the microscope[3] collects even high diffraction orders of the pattern. We determine numerical contrast values from cross sections perpendicular to the stripes of the printed pattern in Figs. 2(g)–2(i). At each point of the cross section the inten-

sity is integrated parallel to the stripes of the pattern [arrow in Fig. 2(f)]. Although the printed pattern (indicated in Fig. 2 bottom, left) does not consist exclusively of parallel stripes the printed area outside the stripes represents less than 5% of the surface and can be neglected. Figures 2(h) and 2(i) demonstrate the expected contrast inversion in the chemical pattern.

$\widetilde{\chi}_{nr}^{(2)}$ is a measure for the adsorbate density. Buck *et al.*[12] and Dannenberger, Buck, and Grunze[13] found in detailed studies that this quantity is related to the interaction of the sulfur group of the thiolate with the Au surface. These and other studies found for metal substrates that $\chi^{(2)}$ changes linearly with adsorbate coverage.[14] The nonlinear optical properties of the interface are either localized on a scale smaller than the distance between adsorbates or they arise from extended regions with the contributions of individual adsorbates remaining linear perturbations. The edge of a macroscopic printed C17–CH3 monolayer exhibits a non-resonant contrast of $\approx 33\%$.[15] Taking this value for calibration we obtain the result that the post-adsorbed regions have a total thiolate coverage, which is $0.21(\pm 0.03)$ ML (with respect to a densely packed phase) lower than the printed regions. This difference can be explained by a less compact structure in which C15–COOH thiolates arrange in agreement with the observation of substantial conformational defects in the alkane backbone, which we concluded from the SFG spectrum, Fig. 1(b).

The vibrational contrast can be calibrated with the spectra of the pure phases (Fig. 1). $\widetilde{\chi}_{res}^{(2)}(\theta)$ is proportional to coverage when no substantial reorientation of the molecules occurs. From the contrast we obtain coverage differences between the postadsorbed and printed regions of $-27(\pm 4)\%$ of a complete C17–CH3 layer and $+43(\pm 5)\%$ of a C15–COOH layer. The latter value takes into account that a small positive peak in the C17–CH3 spectrum [see Fig. 1(a)] enhances the contrast at 2835 cm^{-1}. Contrasts of -100 and $+100\%$ would be expected if the stripes consisted of the pure phases. The evaluation thus reveals that a complete molecular separation is not compatible with observation. The fact that the highest $\widetilde{\chi}_{res}^{(2)}$ values in Figs. 2(h) and 2(i) both do not attain zero but have significant negative values suggests that the molecular species in the pattern are partially mixed during the preparation procedure. These results are systematically observed for samples prepared by the described procedure and are confirmed by local spectra extracted from SFM images taken at each data point of a SFG spectrum.

In conclusion, we demonstrate the ability of SFM to derive quantitative information on different groups of the adsorbed molecules and on the composition of a mixed monolayer by employing electronic and vibrational contrast mechanisms.

[1] H. J. Krause and W. Daum, Appl. Phys. B: Photophys. Laser Chem. **56(1)**, 8 (1993).
[2] M. Flörsheimer, C. Brillert, and H. Fuchs, Mater. Sci. Eng., C **8–9**, 335 (1999).
[3] D. M. P. Hoffmann, K. Kuhnke, and K. Kern, Rev. Sci. Instrum. **73**(9), 3221 (2002).
[4] B. Michel, A. Bernard, A. Bietsch, E. Delamarche, M. Geissler, D. Juncker, H. Kind, J.-P. Renault, H. Rothuizen, H. Schmid, P. Schmidt-Winkel, R. Stutz, and H. Wolf, IBM J. Res. Dev. **45**(5), 697 (2001).
[5] A. Kumar, H. A. Biebuyck, and G. M. Whitesides, Langmuir **10**, 1498 (1994).
[6] F. Schreiber, Prog. Surf. Sci. **65**, 151 (2000).
[7] M. A. Hines, J. A. Todd, and P. Guyot-Sionnest, Langmuir **11**, 493 (1995).
[8] J. Thome, M. Himmelhaus, M. Zharnikov, and M. Grunze, Langmuir **14**, 7435 (1998).
[9] A. L. Harris, C. E. D. Chidsey, N. J. Levinos, and D. N. Loiacono, Chem. Phys. Lett. **141**, 350 (1987).
[10] T. H. Ong, P. B. Davies, and C. D. Bain, Langmuir **9**, 1836 (1993).
[11] A. M. Bittner, M. Epple, K. Kuhnke, R. Houriet, A. Heusler, H. Vogel, A. P. Seitsonen, and K. Kern, J. Electroanal. Chem. **550/551**, 113 (2003).
[12] M. Buck, F. Eisert, J. Fischer, M. Grunze, and F. Träger, Appl. Phys. A: Solids Surf. **53**(6), 552 (1991).
[13] O. Dannenberger, M. Buck, and M. Grunze, J. Phys. Chem. B **103**, 2202 (1999).
[14] F. Eisert, F. Gudmundson, and A. Rosén, Appl. Phys. B: Lasers Opt. **68**, 579 (1999).
[15] D. M. P. Hoffmann, K. Kuhnke, and K. Kern, Proc. SPIE **4812**, 82 (2002).